Continuous Spatio-temporal Atlases of the Asymptomatic and Infarcted Hearts

Pau Medrano-Gracia[1], Brett R. Cowan[1], David A. Bluemke[2], J. Paul Finn[3], Alan H. Kadish[4], Daniel C. Lee[4], João A.C. Lima[5], Avan Suinesiaputra[1], and Alistair A. Young[1]

[1] Dept. Anatomy with Radiology, University of Auckland, New Zealand
{p.medrano,b.cowan,a.suinesiaputra,a.young}@auckland.ac.nz
[2] NIH Clinical Ctr., Bethesda, MD, USA
bluemked@cc.nih.gov
[3] Diagnostic CardioVascular Imaging Section, UCLA, Los Angeles, CA, USA
PFinn@mednet.ucla.edu
[4] Feinberg Cardiovascular Research Inst., Northwestern University, Chicago, IL, USA
{a-kadish,dlee}@northwestern.edu
[5] The Johns Hopkins Hospital, Baltimore, MD, USA
jlima@jhmi.edu

Abstract. Statistical descriptions of regional wall motion abnormalities of the heart are key to understanding both sub-clinical and clinical progression of dysfunction. In this paper we establish a temporal registration framework of the cardiac cycle to build a spatio-temporal atlas of 300 asymptomatic volunteers and 300 symptomatic patients with myocardial infarction. A finite-element model was customised to each person's magnetic resonance images with expert-guided semi-automatic spatial and temporal registration of model parameters. A piece-wise linear temporal registration from user-defined key frames was followed by a Fourier series temporal estimation, providing temporal continuity. All spatial and temporal data were then statistically analysed by means of principal component analysis. Results show differences in sphericity, wall thickening and mitral valve dynamics between the two groups. The modes are available from www.cardiacatlas.org. These atlases can be readily applied to abnormality detection and quantification and can also aid in anatomically constrained shape-based algorithms in automatic planning or segmentation.

1 Introduction

Cardiac magnetic resonance imaging (CMRI) provides detailed spatial and functional information of the human heart. Typically, clinical parameters of interest include endocardial volume, left ventricular (LV) mass, wall thickening and ejection fraction. However, regional wall motion abnormalities are clinically important in the diagnosis and evaluation of regional heart disease such as myocardial infarction. These take the form of spatial variation of temporal characteristics

O. Camara et al. (Eds.): STACOM 2013, LNCS 8330, pp. 143–151, 2014.

which are at present qualitatively assessed by clinicians as being normal or abnormal, for example in determining regional wall motion scores.

Statistical atlases of the heart are, in this context, collections of patient datasets, which can be the images themselves or derived measurements or models which have been registered to a common reference. In this paper we build the latter, i.e. a distribution of regional wall motion in terms of shape and function from two different populations. These atlases are becoming increasingly popular in both the bioengineering [5, 14] and clinical fields [11] since they offer an unprecedented quantitative comparison between a patient and a population. However, to date most atlases have typically focused on specific time points such as end-diastole (ED) and end-systole (ES) and do not usually include all temporal information [10, 12, 13]. In our previous work [14], a similar finite-element model was used however the data and methodology were different. Examples of fully spatio-temporal atlases include [3, 5, 8].

Full coverage of the time domain presents two main challenges, time registration and continuous interpolation. In this paper we address these two challenges and present an asymptomatic and symptomatic spatio-temporal atlas through their modes of variation. The main contributions of this paper are:

1. A compact representation of the spatio-temporal variation of regional wall motion in terms of a parametric model with a relatively small number of parameters
2. Application to a reasonably large number of asymptomatic and symptomatic cases
3. Identification of clinically important shape indicators including sphericity and wall thickening in the symptomatic vs. asymptomatic groups.

2 Data and Methods

Image data were obtained using the Cardiac Atlas Project [6] from two clinical studies: the Multi-Ethnic Study of Atherosclerosis (MESA) study [1] for the asymptomatic cohort and the Defibrillators To Reduce Risk By Magnetic Resonance Imaging Evaluation (DETERMINE) clinical trial [9] for the symptomatic sample. Three hundred cases were randomly selected from each study. A typical dataset comprised 20-30 frames in 6-8 short-axis slices and 3-4 long-axis slices (imaging parameters can be found in [1, 9]). All images were acquired using prospective electrocardiogram gating and therefore cover the entire cycle.

At the time of recruitment, the MESA study protocol ensured that participants did not have clinical evidence of heart attack, angina, stroke, heart failure or atrial fibrillation [1]. The DETERMINE study was designed as a prospective, multi-centre, randomised, clinical trial in patients with coronary artery disease and mild-to-moderate LV dysfunction [9].

Guide-point modelling [19] was used to adaptively optimise a time-varying 3D finite-element model of the LV to fit each subject's images using custom software (CIM version 6.0, Auckland, New Zealand). The model was interactively fitted to "guide points" provided by the analyst, as well as computer-generated

data points calculated from the image using an edge detection algorithm by linear least-squares. The typical time of analysis for a trained expert varied between 24-35 minutes. This finite-element representation enabled a succinct parametrisation with anatomical correspondence across subjects. The spatial representation comprised 215 Bézier parameters ($i = 1 \ldots 215$) which governed the shape of the endocardial and epicardial surfaces [16]. These parameters were expressed in prolate spheroidal coordinates in terms of focal length f (overall scaling) and radial λ_i, hyperboloidal μ_i and azimuthal θ_i coordinates for each control point.

2.1 Temporal Analysis

Functional analysis of the time-varying data [18] comprised two main steps:

1. **Temporal Registration.** Since the number of frames varied with subject, a temporal registration step was needed to ensure that all cases conformed to a common normalised temporal reference (2.1.1).

2. **Temporal Continuity.** A continuous extension through time is desirable for data smoothing, continuity and applying dimension reduction techniques in the time domain. This enables sampling of the models at any time point in the cardiac cycle (2.1.2).

Once these two challenges are overcome, the statistical analysis of linear modes of variation can be written in terms of perturbations about the mean, either for any arbitrary time-point $t = t_i$ in the cardiac cycle (thus becoming static), or by coupling all time variability (discussed in 2.2).

2.1.1 Temporal Registration

To align all cases to a common temporal reference, a time warp from the discrete frame space ($f = 0, 1, 2, \ldots, f_i, \ldots, F$) to a normalised cardiac cycle $[0, 1]$ was constructed such that $t = 0$ represented the ED frame and $t = 0.35$ represented the ES frame (f_{ES}). The normalised time coordinate of 0.35 was chosen for ES because this is the typical normal duration of systole in normal people [7]. This defines a periodic time reference where the warped discrete points $t_i \in [0, 1]$ are given by:

$$t_i = \begin{cases} 0.35\dfrac{f_i}{f_{ES}} & \text{for } t_i \leq f_{ES} \\ 0.35 + 0.65\dfrac{f_i - f_{ES}}{F - f_{ES} + 1} & \text{for } t_i > f_{ES} \end{cases} \tag{1}$$

2.1.2 Temporal Continuity

The Fourier series is a natural representation for our periodic data [2]. Not only does it provide a continuous description of function but it also conveniently

represents our function with a small number of coefficients (if we accept some error due to loss of high frequencies).

The Fourier partial sums for any periodic function $f(t)$ at least $\mathcal{L}^1$-integrable in $[-\pi, \pi]$ are

$$(S_N f)(t) = \frac{a_0}{2} + \sum_{n=1}^{N} \left(a_n \cos(nt) + b_n \sin(nt)\right) \quad N \geq 0,$$

where $a_n = \frac{1}{\pi} \int_{-\pi}^{\pi} f(t) \cos(nt)\, dt\, (n \geq 0)$ and $b_n = \frac{1}{\pi} \int_{-\pi}^{\pi} f(t) \sin(nt)\, dt\, (n \geq 1)$.

In our case, the cycle occurs in $[0, 1]$ and we fix the number of harmonics to $N = 5$ which yields 11 coefficients. This has been shown previously to give acceptable error with respect to a high frame rate (60 fps) standard [20].

We therefore have:

$$(S_5 f)(t) = \frac{a_0}{2} + \sum_{n=1}^{5} \left(a_n \cos(2\pi nt) + b_n \sin(2\pi nt)\right)$$

where $a_n = 2 \int_0^1 f(t) \cos(2\pi t)\, dt\, (n \geq 0)$ and $b_n = 2 \int_0^1 f(t) \sin(2\pi t)\, dt\, (n \geq 1)$.

Given that $f(t)$ must be integrable in $[0, 1]$ and that the available data is discrete with non-uniform spacing (due to the temporal registration), $f(t)$ was chosen to be a cubic B-spline [4] supporting all time-registered points from 2.1.1. This enabled efficient integration by quadrature using QUADPACK [17].

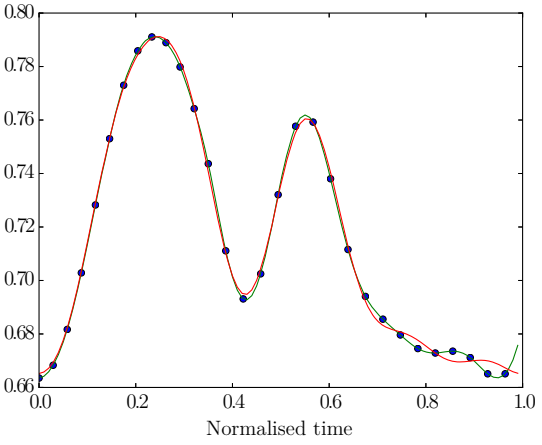

Fig. 1. Example of a $\lambda_i(t)$ parameter. The blue dots represent the time-registered $\lambda_i(t_j)$ points at each frame, the green line the cubic B-spline, and the red line the Fourier partial sums with 5 harmonics $(S_5 f)$.

Figure 1 shows an example of this approximation which leads to two important remarks:

1. By construction, the B-spline function (in green) goes through all available time-points whereas the Fourier approximation $S_5 f$ (in red) can only approximate them since the number of degrees of freedom is smaller than the number of time-points ($11 < 30$ in this particular example)
2. $S_5 f$ is continuously periodic at the boundaries of $[0, 1]$.

Henceforth, for each one of the spatial shape parameters, we use the corresponding $(S_5\lambda_i)(t)$ as the continuous and smooth temporal extension of our data for statistical time analysis.

2.2 4D Modes of Variation

In order to analyse spatio-temporal variation, two scenarios were built. Let B be the data matrix where the rows represent the different variables and the columns different observations. In our case the variables are the model parameters and the number of observations is $N_1 = 300$ for DETERMINE and $N_2 = 300$ for MESA. Let B_c be a single observation column of B. The first scenario (these results are available on-line[1]) is to simply treat time independently, thus resulting in a variance analysis at a standard sampling of $t \in [0, 1]$, e.g. for ED $B_c^T = [\lambda_1(t_{ED})\, \lambda_2(t_{ED})\, \lambda_3(t_{ED})\, \cdots]$, and for ES $B_c^T = [\lambda_1(t_{ES})\, \lambda_2(t_{ES})\, \lambda_3(t_{ES})\, \cdots]$.

The second scenario, and the one we focus on for the remainder of this paper, is to investigate the spatio-temporal parametric variance. To this end, all 11 Fourier coefficients were coupled into a single vector or column of B. Following the notation in 2.1.2, we then have

$$B_c^T = \left[\underbrace{a_0^{\lambda_1}\, a_1^{\lambda_1}\, b_1^{\lambda_1}\, a_2^{\lambda_1}\, b_2^{\lambda_1}\, \ldots\, a_5^{\lambda_1}\, b_5^{\lambda_1}}_{a_0+5 \text{ harmonics}} \quad a_0^{\lambda_2}\, a_1^{\lambda_2}\, b_1^{\lambda_2}\, a_2^{\lambda_2}\, b_2^{\lambda_2}\, \ldots\, a_5^{\lambda_2}\, b_5^{\lambda_2}\, \cdots \right]$$

where for each parameter of the LV model, we have 11 coefficients which carry *most* of the temporal information. This can be interpreted as a multi-variate analysis in shape and time (function) simultaneously, taking advantage of the full physiological information of the finite-element model.

Typically one is only interested in the first few modes of variation, i.e. those which portray most statistical variability. The number of modes that should be kept is a broad topic of research [15] and is dependent on the application.

Figure 2 and Figure 3 show the first three PCA modes of variation for the coupled temporal analysis when using all prolate spheroidal parameters except the focal length (f) for the asymptomatic and symptomatic datasets. To capture 90% of total variation, 22 modes were required for the MESA dataset, whereas the DETERMINE dataset required 27. Temporal animations of these modes and lower-variance modes can be seen on-line[1].

[1] `http://www.cardiacatlas.org/web/guest/modes`

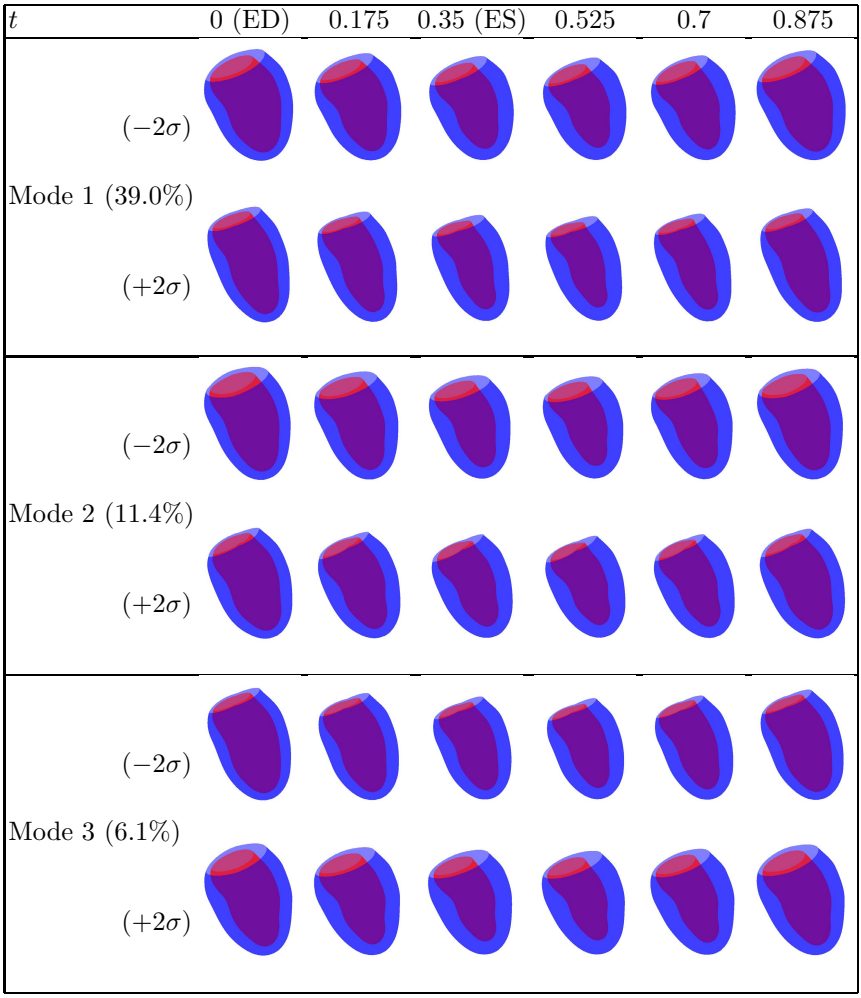

Fig. 2. Asymptomatic (MESA) Fourier temporal modes for all variable prolate spheroidal parameters except focal length (56.5% of variability shown). Slightly elevated anterior view (septum on the left).

3 Discussion

In the MESA or asymptomatic modes of variation in Figure 2, it could be reasoned that the first mode corresponds to the lengthening component of the ventricle, and modes 2 and 3 correspond to features of the mitral valve geometry and base plane tilt. However, from an overall geometric or clinical perspective, there are no *pure* modes of variation, e.g. only sphericity.

In the DETERMINE or symptomatic (infarct) modes in Figure 3, mode 1 represents the sphericity (as was also found in a previous static analysis [13]),

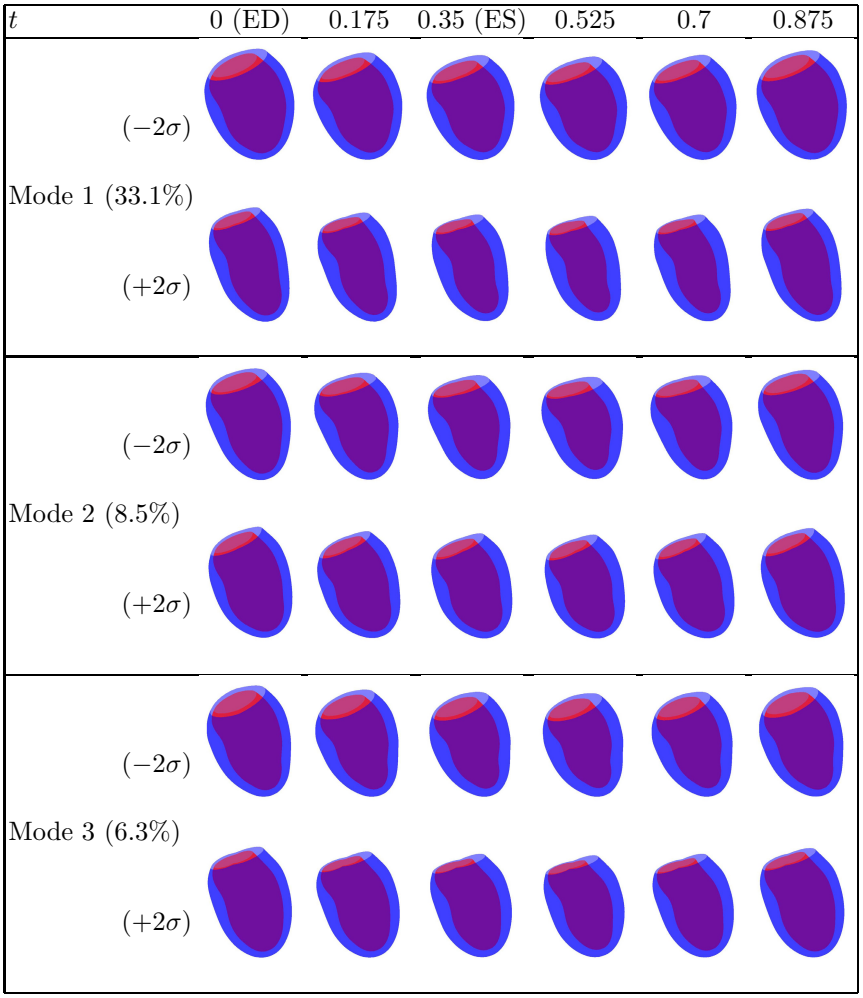

Fig. 3. Symptomatic (DETERMINE) Fourier temporal modes for all variable prolate spheroidal parameters except focal length (47.9% of variability shown). Slightly elevated anterior view (septum on the left).

mode 2 the lower mid-ventricular thickness, mode 3 shows mitral valve geometry features along with a rounding or *bulging* of the apical region. These features correlate well with clinical indicators of heart failure, i.e. sphericity, wall thinning and local dilation of the ventricle are features of infarcted models.

When comparing the modes of variation in Figures 2 and 3 with their static counterparts (available on-line[1]), the first characteristic that becomes apparent is the similarities of the temporal modes with the static counterparts. This implies that the time variability is in itself lesser than the shape variability.

The quantification of these shape and function differences —by projecting onto the atlas modes— enable detection and classification of abnormality by using statistical distances such as Mahalanobis or Bhattacharyya (current ongoing research in our team).

Acknowledgements. The work described was supported by Award Number R01HL087773 from the National Heart, Lung, and Blood Institute (NHLBI). The content is solely the responsibility of the authors and does not necessarily represent the official views of the NHLBI or the National Institutes of Health (NIH). MESA was supported by contracts N01-HC-95159 through N01-HC-95169 from the NHLBI and by grants UL1-RR-024156 and UL1-RR-025005 from the National Center for Research Resources. The NIH (5R01HL091069) and St. Jude Medical provided grant support for the DETERMINE trial.

References

[1] Bild, D., Bluemke, D., Burke, G., Detrano, R., Diez Roux, A., Folsom, A., Greenland, P., et al.: Multi-ethnic study of atherosclerosis: objectives and design. American Journal of Epidemiology 156(9), 871 (2002)

[2] Brown, J., Churchill, R.: Fourier series and boundary value problems. Recherche 67, 2 (1993)

[3] Chandrashekara, R., Rao, A., Sanchez-Ortiz, G.I., Mohiaddin, R.H., Rueckert, D.: Construction of a statistical model for cardiac motion analysis using nonrigid image registration. In: Taylor, C.J., Noble, J.A. (eds.) IPMI 2003. LNCS, vol. 2732, pp. 599–610. Springer, Heidelberg (2003)

[4] Dierckx, P.: Curve and surface fitting with splines. Oxford University Press, USA (1995)

[5] Duchateau, N., De Craene, M., Piella, G., Silva, E., Doltra, A., Sitges, M., Bijnens, B., Frangi, A.: A spatiotemporal statistical atlas of motion for the quantification of abnormal myocardial tissue velocities. Medical Image Analysis 15(3), 316–328 (2011)

[6] Fonseca, C., Backhaus, M., Bluemke, D., Britten, R., Do Chung, J., Cowan, B., Dinov, I., Finn, J., Hunter, P., Kadish, A., et al.: The Cardiac Atlas Project – an imaging database for computational modeling and statistical atlases of the heart. Bioinformatics (2011)

[7] Guyton, A., Hall, J.: Medical Physiology. Saunders, Philadelphia (2000)

[8] Hoogendoorn, C., Duchateau, N., Sánchez-Quintana, D., Whitmarsh, T., Sukno, F., De Craene, M., Lekadir, K., Frangi, A.: A high-resolution atlas and statistical model of the human heart from multislice CT. IEEE Transactions on Medical Imaging (2013)

[9] Kadish, A., Bello, D., Finn, J., Bonow, R., Schaechter, A., Subacius, H., Albert, C., Daubert, J., Fonseca, C., Goldberger, J.: Rationale and design for the defibrillators to reduce risk by magnetic resonance imaging evaluation (DETERMINE) trial. Journal of Cardiovascular Electrophysiology 20(9), 982–987 (2009)

[10] Kaus, M.R., von Berg, J., Niessen, W.J., Pekar, V.: Automated segmentation of the left ventricle in cardiac MRI. In: Ellis, R.E., Peters, T.M. (eds.) MICCAI 2003. LNCS, vol. 2878, pp. 432–439. Springer, Heidelberg (2003)

[11] Lewandowski, A.J., Augustine, D., Lamata, P., Davis, E.F., Lazdam, M., Francis, J., McCormick, K., Wilkinson, A., Singhal, A., Lucas, A., et al.: The preterm heart in adult life: Cardiovascular magnetic resonance reveals distinct differences in left ventricular mass, geometry and function. Circulation (2012)
[12] Lötjönen, J., Kivistö, S., Koikkalainen, J., Smutek, D., Lauerma, K.: Statistical shape model of atria, ventricles and epicardium from short-and long-axis MR images. Medical Image Analysis 8(3), 371–386 (2004)
[13] Medrano-Gracia, P., Cowan, B., Finn, J., Fonseca, C., Kadish, A., Lee, D., Tao, W., Young, A.: The cardiac atlas project: preliminary description of heart shape in patients with myocardial infarction. Statistical Atlases and Computational Models of the Heart, 46–53 (2010)
[14] Medrano-Gracia, P., Cowan, B.R., Bluemke, D.A., Finn, J.P., Lima, J.A.C., Suinesiaputra, A., Young, A.A.: Large scale left ventricular shape atlas using automated model fitting to contours. In: Ourselin, S., Rueckert, D., Smith, N. (eds.) FIMH 2013. LNCS, vol. 7945, pp. 433–441. Springer, Heidelberg (2013)
[15] Mei, L., Figl, M., Darzi, A., Rueckert, D., Edwards, P.: Sample sufficiency and PCA dimension for statistical shape models. In: Forsyth, D., Torr, P., Zisserman, A. (eds.) ECCV 2008, Part IV. LNCS, vol. 5305, pp. 492–503. Springer, Heidelberg (2008)
[16] Nielsen, P., Le Grice, I., Smaill, B., Hunter, P.: Mathematical model of geometry and fibrous structure of the heart. American Journal of Physiology- Heart and Circulatory Physiology 260(4), H1365 (1991)
[17] Piessens, R., Doncker-Kapenga, D., Überhuber, C., Kahaner, D., et al.: QUADPACK, a subroutine package for automatic integration. Springer (1983)
[18] Ramsay, J.: Functional data analysis. Wiley Online Library (2006)
[19] Young, A., Cowan, B., Thrupp, S., Hedley, W., Dell'Italia, L.: Left ventricular mass and volume: Fast calculation with guide-point modeling on MR images. Radiology 216(2), 597 (2000)
[20] Young, A.A., Hunter, P.J., Smaill, B.H.: Estimation of epicardial strain using the motions of coronary bifurcations in biplane cineangiography. IEEE Transactions on Biomedical Engineering 39(5), 526–531 (1992)